THE JOURNAL OF PHYSICAL CHEMISTRY Letters

Letter

pubs.acs.org/JPCL

Enhanced Magnetic Anisotropy via Quasi-Molecular Magnet at Organic-Ferromagnetic Contact

Yao-Jane Hsu,*[,†,∥] Yu-Ling Lai,[†] Chih-Han Chen,[†] Ying-Chang Lin,[†] Hsiu-Yun Chien,[‡] Jeng-Han Wang,*[,‡] Tu-Ngoc Lam,[§] Yuet-Loy Chan,[†] D. H. Wei,[†] Hong-Ji Lin,[†] and Chien-Te Chen[†]

[†]National Synchrotron Radiation Research Center, Hsinchu, 30076, Taiwan, R.O.C.

[‡]Department of Chemistry, National Taiwan Normal University, Taipei, 11677, Taiwan, R.O.C.

[§]Institute of Nano Technology, National Chiao Tung University, Hsinchu, 30010, Taiwan, R.O.C.

[∥]Department of Photonics, National Cheng Kung University, Tainan 701, Taiwan, R.O.C.

Supporting Information

ABSTRACT: To realize the origin of efficient spin injection at organic-ferromagnetic contact in organic spintronics, we have implemented the formation of quasi-molecular magnet via surface restructuring of a strong organic acceptor, tetrafluoro-tetracyano-quinodimethane (F4-TCNQ), in contact with ferromagnetic cobalt. Our results demonstrate a spin-polarized F4-TCNQ layer and a remarkably enhanced magnetic anisotropy of the Co film. The novel magnetic properties are contributed from strong magnetic coupling caused by the molecular restructuring that displays an angular anchoring conformation of CN and upwardly protruding fluorine atoms. We conclude that the π bonds of CN, instead of the lone-pair electrons of N atoms, contribute to the hybridization-induced magnetic coupling between CN and Co and generate a superior magnetic order on the surface.

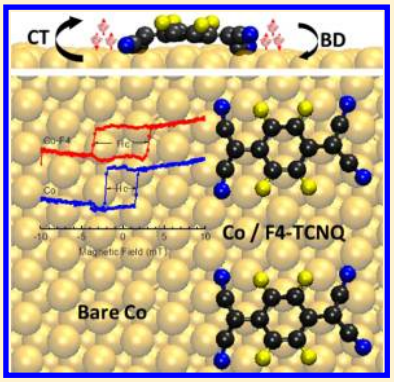

SECTION: Surfaces, Interfaces, Porous Materials, and Catalysis

Organic spintronics with integrated organic electronics have the potential to produce multifunctional devices of which the electronic structures and spin degrees of freedom are tailored with organic functional groups. With an enduring spin coherence and large distance through weak spin−orbit coupling and hyperfine interaction (HFI), the efficacy of manipulating, with organic molecules, the spin state and the interaction with a magnetic field offers a new and tantalizing approach toward molecular spintronics.[1−4] On the basis of these, giant magnetoresistance (GMR) has been measured in organic spin valve devices for orgainc thick films or thin tunnel junctions.[1,5,6] To ensure long spin coherence with time and distance for the spin injection/transport in organic spintronic devices, the spin scatterings caused by spin−orbit, HFIs, or other effects still need to be taken into account. Although most organic semiconductors are composed of light elements, the spin−orbit interaction sometimes still plays a crucial role to affect the spin-relaxation time and, consequently, spin diffusion length in magnetoresistance.[7,8] Besides, the HFI plays an important role in organic magnetotransport for determining the spin−lattice relaxation time or influence the spin response in optically detected magnetic resonance.[9−11] The device performance of organic spintronics therefore may be enhanced simply by manipulating these interaction between the organic spacer and magnetic electrodes.

Interfaces between a ferromagnetic electrode and an organic material are known to affect critically the efficiency of spin injection or detection.[12−16] For example, efficient spin injection was illustrated through spin-polarized Alq_3 via hybridized states between the nitrogen of a quinoline ligand and Fe.[17] In addition, an insertion of a LiF polar layer was found to be capable of manipulating the spin band at an organic−ferromagnetic interface.[13] A fundamental understanding of how interfacial properties engineer the surface spin polarization[17−19] might facilitate the spin injection and transport and the design of the local spin polarization at an interface.[20] The fluorinated TCNQ-analog molecule, tetrafluoro-tetracyano-quinodimethane (F4-TCNQ), is a strong electron acceptor that is commonly utilized to diminish the injection barrier for holes by forming an interfacial dipole layer at the metal−organic contact.[21] When coevaporated or doped with electron-donor molecules in organic devices or thin films, the device performance or conductivity is significantly improved.[22,23] The amelioratation not only arises from electronic modification at the interface but also involves charge redistribution led by structural rearrangements.[24,25]

Moreover, tetracyano-based molecules are promising materials to form high-temperature metal−organic magnets.[26,27] The interplay proceeding via electron transfer between the metal

Received: October 31, 2012
Accepted: December 19, 2012
Published: December 19, 2012

and the tetracyano-based ligands can exhibit magnetic order well above 300 K. The tactics of manipulating magnetic coupling between molecules with tetracyano-base ligands and ferromagnetic metals is hence foreseen to realize the spin injection and transport in spintronics. Additionally, the charge-transfer-induced magnetic properties effect has successfully been demonstrated on organic−inorganic interface, like cooperative molecular field of self-assembly monolayers containing chiral dipolar structures on metallic surfaces.[28] For these reasons, we investigated the magnetic coupling of F4-TCNQ on a Co surface in terms of the molecular binding and anchoring structure. Because an anchoring structure of organic molecules on metal electrodes strongly influences the electronic configuration[29] and thus the device conductance,[30] it should be prudently considered that the interfacial spin injection is affected by the corresponding anchoring structure. This anchoring structure on electrodes is generally determined by the substrate, the rate of deposition, temperature, surface roughness, and so on. Such influential factors and correlations should be taken into account in fabricating spintronic devices. We therefore expect that the local spin design to implement the molecular restructuring-assisted spin polarization based on a strong donor−acceptor pair can optimize the spin injection and transport in organic spintronics and pave the way toward highly efficient organic molecular spintronics.

The chemical states characterized with XPS and NEXAFS of F4-TCNQ of varied thickness on Co are reported in Figure 1. The N 1s XPS in Figure 1a exhibits three lines; their binding energies (BEs) are 398.0, 398.9, and 399.8 eV. By analogy to the results of F4-TCNQ and TCNQ reported on other metal surfaces,[31−33] we assigned the N 1s line at 398.0 eV to an anionic species resulting from charge transfer (in direct contact with Co) and the line at 398.9 eV to noncontact CN or neutral F4-TCNQ (multiple layers). The line centered at 399.8 eV and having a satellite or shakeup structure was initially suppressed with the presence of metal at thin F4-TCNQ but became perceptible upon increased thickness. These N 1s results signal a significant charge transfer from Co to F4-TCNQ at a thin coverage through the presence of the line evident at 398.0 eV. Thickness-dependent N *K*-edge NEXAFS was recorded to confirm the charge transfer. In Figure 1b, the line at 396.2 eV is attributed to the second-order effect of L_2-edge absorption from underlayer Co. For a thickness less than 0.5 nm, the spectra show initially two absorptions at 398.5 and 399.4 eV due to two orthogonal π^* orbitals of the CN group, which lie near one another in the neutral molecule but become significantly split in the charged state.[33−35] With further F4-TCNQ on Co, these two lines gradually merge into a broad line, centered at 399.2 eV with a slight shoulder at 398.5 eV, and display saturated intensities at thickness 2−10 nm.

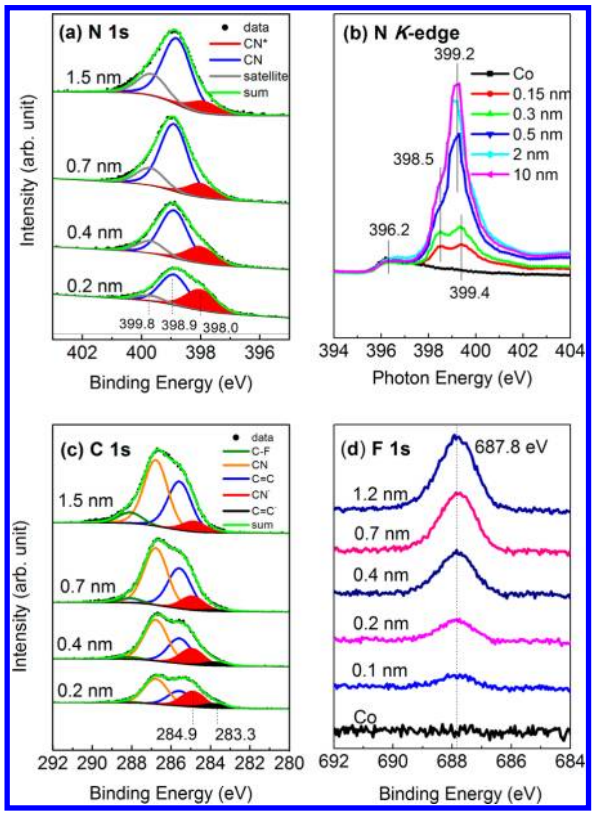

Figure 1. Charge transfer for F4-TCNQ in contact with Co. (a) XPS spectra of N 1s. (b) N *K*-edge NEXAFS spectra as a function of F4-TCNQ thickness. (c) XPS spectra of C 1s and (d) F 1s of F4-TCNQ on cobalt as a function of F4-TCNQ thickness. The incident photon energy is 480 eV for N 1s and C 1s and 900 eV for F 1s XPS.

The corresponding C 1s XPS, shown in Figure 1c, is deconvoluted into multiple features to represent carbon atoms in varied environments in F4-TCNQ. The lines centered at 288.1, 286.8, and 285.6 eV are associated with CF, CN, and C═C in the molecular adsorption of F4-TCNQ, respectively. The lines at BE 284.9 and 283.8 eV are attributed to anionic CN and C═C, respectively, in the central quinone ring through the charge transfer. From these data, we found that the anionic C═C of central ring shows a closed interaction with Co substrate. This behavior is different from the restructuring of F4-TCNQ on coinage metals,[24,25] which display a distant central ring from substrate. This dissimilarity might imply a distinct anchoring structure on Co surface. In addition, unlike N 1s and C 1s spectra, the F 1s XPS shown in Figure 1d displays a BE at 687.8 eV that is invariant with thickness of deposited F4-TCNQ; this constant BE indicates that the fluorine atoms are not involved in the charge transfer. The details regarding the role of the large electron affinity of fluorine atoms are discussed in the following on polarized NEXAFS spectra and the DFT calculation.

As depicted in core-level PES and NEXAFS spectra, the valence-level PES (Figure 2a) shows new interfacial electronic states corresponding to a charge transfer from Co 3d to the LUMO of F4-TCNQ in the BE range 1 to 2 eV. With increasing thickness of F4-TCNQ, the extension of the Fermi range (Figure 2b) indicates that the interfacial states shift to large BE and diminish for a thick F4-TCNQ deposit. These charge-transfer states correspond consistently to those observed for F4-TCNQ/Au[32] and Na-doped F4-TCNQ[34] and conform to the characterization derived from core-level PES and NEXAFS spectral results. The line centered 6−8 eV below the FE of thin F4-TCNQ layers (0.05−1.0 nm) in Figure 2a exhibits a BE larger than that of thick layers (2.0−5.0 nm), whereas the other peaks corresponding to deep molecular orbitals (MOs) have constant BE. This BE shift is not typical in general because the charge transfer is involved in the valence states near Fermi level. The contrary BE shift in comparison with that near Fermi range implies the scenario of strong coupling between Co d band and CN π orbital that lowers down the energy state of CN π orbital upon adsorption, as confirmed from our DOS analysis. The variation of PES in the range 6−8 eV in Figure 2a that presents an opposite BE shift

dx.doi.org/10.1021/jz301757x | J. Phys. Chem. Lett. 2013, 4, 310−316

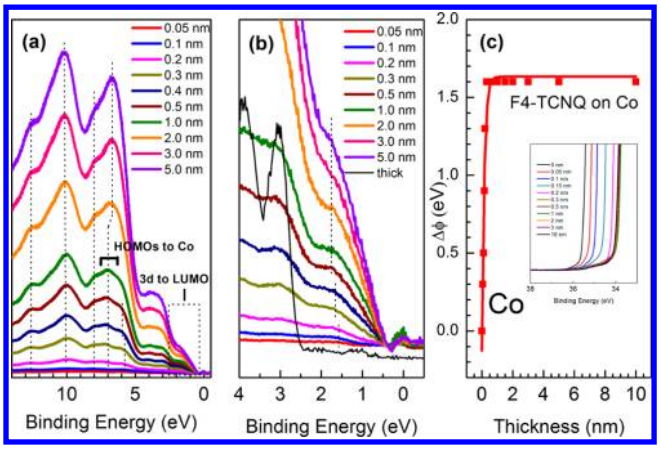

Figure 2. Valence electronic structures of F4-TCNQ on Co: (a) valence-level PES spectra for F4-TCNQ of varied thickness on cobalt. To avoid d band interference from Co, the pristine Co spectrum (scaled to the intensity at EF) is subtracted from all spectra. (b) Enlarged region near the Fermi EF spectra in part a. (c) Variation of work function $\Delta\phi$ with thickness of F4-TCNQ on cobalt. The inset shows the secondary electron cutoff region (at sample bias −4 V).

valid only for direct contact between F4-TCNQ and Co signifies a back-donation from CN π orbital to Co.[24] On the basis of the PES and NEXAFS spectral results, we suggest that charges not only transfer from Co to LUMOs but also return from CN π orbital to Co. This bidirectional charge transfer resembles the behavior of bonding and backbonding properties generally found in organic magnets.[27] In addition to the strong interaction as a quasi-molecular magnet, a change of work function (Figure 2c) is observed from 4.5 to 6.1 eV, which corresponds to a large dipole on the surface.[21] This surface dipole layer is capable of tuning energy levels for interfacial band alignments in organic spintronics and hence anticipated to affect relative probabilities of transfer of spin-up and spin-down charge carriers from organics to ferromagnetic electrodes.

To investigate the origin of an efficient charge transfer, we examined the conformation and bonding geometry of F4-TCNQ on cobalt with polarized N and C *K*-edge absorption spectra. The experimental configuration of polarized NEXAFS shown in Figure 3a displays a linear polarization with electric field parallel (denoted as s-polarization) or perpendicularly (p-polarization), irradiating the sample to determine the molecular anchoring orientation on the surface. In Figure 3b, the two lines that originating from two π^* orbitals split due to interaction with Co for the N absorption edge (as shown in Figure 2b and explained above) display evident polarization dichroism. The incidence of p-polarization on the sample enhances the absorption line at 399.3 eV, whereas the s-polarization intensifies the line at 398.5 eV. The reversed polarization dependence indicates that CN has a preferred bonding structure.[36] By analyzing the intensity ratio (I_s/I_p) for the s- and p-polarization of these resonances, we determined the bonding geometry of CN group. The bonding angle is estimated to be ~30° from the surface; this angle (larger than the tilted angle 10−20° of CN for TCNQ on Cu(100)[37]) reveals a distinct bent downward structure because of a strong interaction between CN and Co. The polarized C *K*-edge NEXAFS spectra of F4-TCNQ (0.3 and 0.5 nm) shown in Figure 3c,d display several fine features (most from π^* absorption) below 290 eV and several broad lines to σ^* transitions above 290 eV. The features at 285.6 and 286.8 eV are associated with the C 1s transition of CN and of the quinone ring to unoccupied MO, respectively. As expected, these two π^* orbitals display opposite polarization dependences

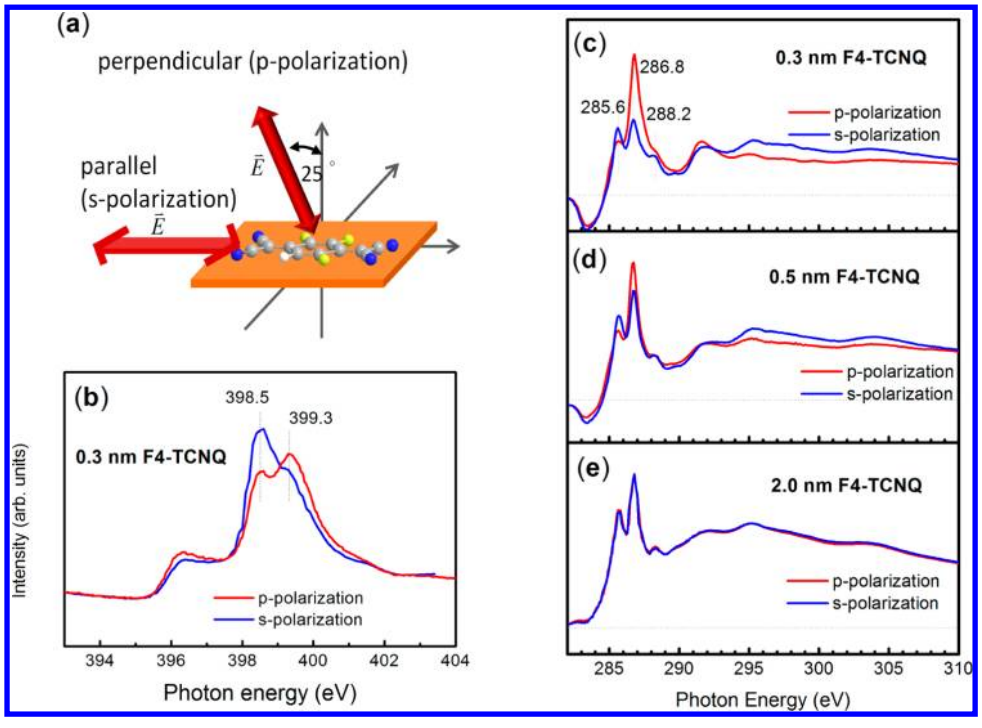

Figure 3. Molecular restructuring of F4-TCNQ. (a) Schematic of experimental geometry of polarized NEXAFS. (b) Linearly polarized nitrogen *K*-edge NEXAFS spectra of F4-TCNQ (0.3 nm). Linearly polarized carbon *K*-edge NEXAFS spectra of F4-TCNQ at thickness (c) 0.3, (d) 0.5, and (e) 2.0 nm on cobalt. The p-polarization denotes an electric field of the incident photons perpendicular to the sample surface, and s-polarization denotes an electric field parallel to the sample surface.

dx.doi.org/10.1021/jz301757x | *J. Phys. Chem. Lett.* 2013, 4, 310−316

because of the distinct bent downward structure. The resonance at 286.8 eV and the σ^* resonances above 290 eV also exhibit contrary polarization dependences, indicating that the central quinone ring exhibits a conformation preferably lying flat on the surface. In brief, these two reversed dependences indicate that the CN bonds in absorbed flat-lying F4-TCNQ are in an angular conformation because of the enhanced structural freedom resulting from the altered bonding character on the charge transfer. With F4-TCNQ growth to thickness 2 nm in Figure 3e, the polarization dependence vanished, indicating that the structure no longer has a preferred angular structure in the multilayers because of the decreased interaction with Co.

To discriminate and to account for the charge distribution and structure rearrangement, Figure 4a,b illustrates optimized geometries with bonding through N atoms and CN groups for F4-TCNQ on Co(111) in side views, respectively. Their corresponding geometries in top views are displayed in Figure 4c,d. According to the DFT calculation, the latter structure with CN groups bound (through π electrons) tightly to the hollow sites of Co surface has a greater adsorption energy (~1.6 eV larger) than that of the former structure, which has been reported on Cu(111) surface,[24] with N atoms (through lone-pair electrons) on top of Co atoms. The analysis of charges induced upon adsorption

$$\Delta\rho = \rho(\text{adsorption}) - \rho(\text{surface}) - \rho(\text{adsorbate})$$

of each bonding CN group and the quinone ring is −0.6 and −0.8 |e|, respectively, for the CN-bonding structure (Figure 4b). The acquired charges are more localized at the CN group and the quinone ring than those in the N-bonding structure (Figure 4a). This analysis is consistent with the above results of the C and N 1s XPS. In the side view of Figure 4b, three CN groups (blue) show an inclination bonding to the Co surface (yellow), but all fluorine atoms protrude farther away from the surface, confirming the observation of the invariant F 1s XPS. This adsorption structure (Figure 4b) also agrees well with the experimentally observed charge transfer that occurs mainly on CN groups and the quinone ring; the distant fluorine atoms are not involved in the charge transfer. From a comparison with the former restructuring,[24,37] we deduce that the structure (Figure 4b) with π electrons of CN, instead of the lone-pair electrons of N atoms (Figure 4a), contributes to the hybridization with Co. To explore the relation between restructuring and magnetic coupling, we analyze the spin-polarized DOS for varied anchoring configurations mentioned above (Figure 4e). The DOS demonstrates a spin density disparity near FE for adsorbed CN, especially the most evident at 2.2−2.6 eV above the FE, from which we infer that F4-TCNQ through the orbital hybridization between CN and Co might be spin-polarized via restructuring-assisted charge transfer,[18] but the anchoring in the arch bridge through N atoms has no such spin density asymmetry. In addition, we observed moderate spin density disparity below FE 0−3.0 eV for structure 4b, whereas it is more symmetrical for structure 4a. As a result, the structure 4b bonding to Co through CN π electrons ameliorates F4-TCNQ molecule to be spin-polarized and facilitates the spin-injection and transport into organic layers.

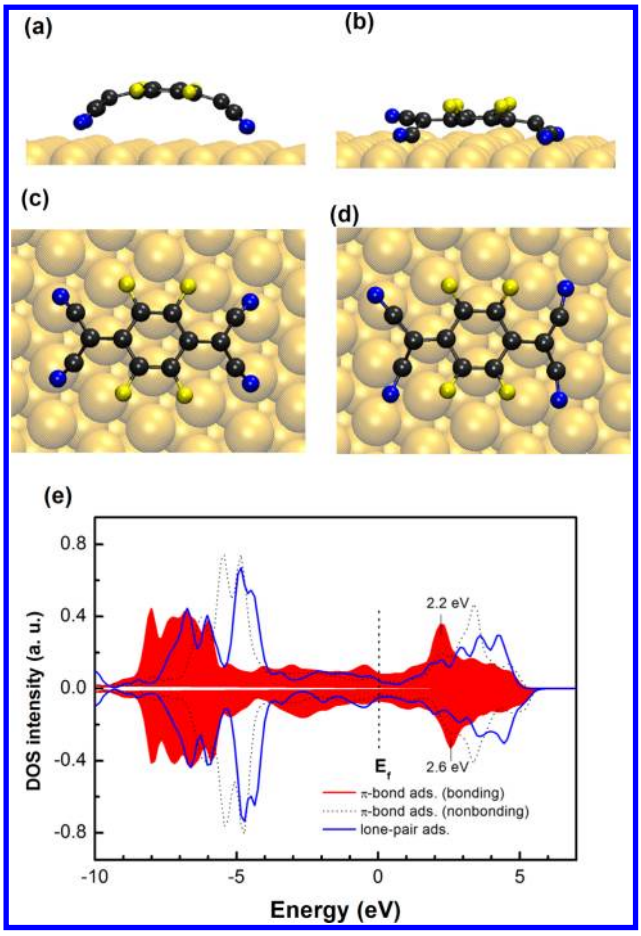

Figure 4. Anchoring-structure-dominated spin-polarization. (a) Top and (c) side views of an adsorbed F4-TCNQ molecule through lone pair electrons of N atoms anchoring on Co(111) in an optimized conformation, shown with C black, N blue, F yellow, and Co golden spheres. (b) Top and (d) side views of an adsorbed F4-TCNQ molecule on Co(111) via π bonds of CN. (e) Corresponding spin-polarized DOS of an anchored configuration of panels a and b on a Co surface, respectively. The structure 4b through π bonding with Co ameliorates F4-TCNQ molecule to be spin-polarized.

The surface spin polarization is a crucial issue to establish efficient spin injection and transport at the organic-ferromagnetic interface. The above calculation indicates that a surface spin polarization might occur for F4-TCNQ with an enormous angular restructuring on Co (Figure 4b). For this reason, we verified whether F4-TCNQ is spin-polarized on ferromagnetic Co. Surface-sensitive XMCD, a unique probe for magnetic properties, with average probing depth 5−9 nm[38] was implemented to inspect the surface spin polarization. Figure 5 shows the Co *L*-edge and N *K*-edge XMCD spectra acquired from Co/F4-TCNQ (1.5 nm) near 300 K with magnetic field $H = 10^{-2} \sim 5 \times 10^{-3}$ Tesla (T) applied at a configuration in-plane ($\theta = 0°$) for a parallel (I^+) and an antiparallel (I^-) alignment to the photon. After deposition of F4-TCNQ, the cobalt film (thickness 3.4 nm) displayed a strong in-plane magnetization (Figure 5a), similar to that of a bare Co film that expressed an easy axis oriented azimuthally along [110] and [−1−10] directions. To realize the influence of the F4-TCNQ adsorption on the ferromagnetic properties, we normalized the XAS intensity for both films to compare the XMCD signals ($I^- - I^+$). The XMCD spectrum of Co/F4-TCNQ film presents an intensity similar to, but smaller than, that of the bare Co film (the dichroic ratio defined as $[(I^- - I^+)/(I^- + I^+)]$ is estimated to be 19% for bare Co and 16% for deposited F4-TCNQ), revealing that the magnetic moment of the Co film is slightly decreased upon F4-TCNQ adsorption. According to the DFT

dx.doi.org/10.1021/jz301757x | J. Phys. Chem. Lett. 2013, 4, 310−316

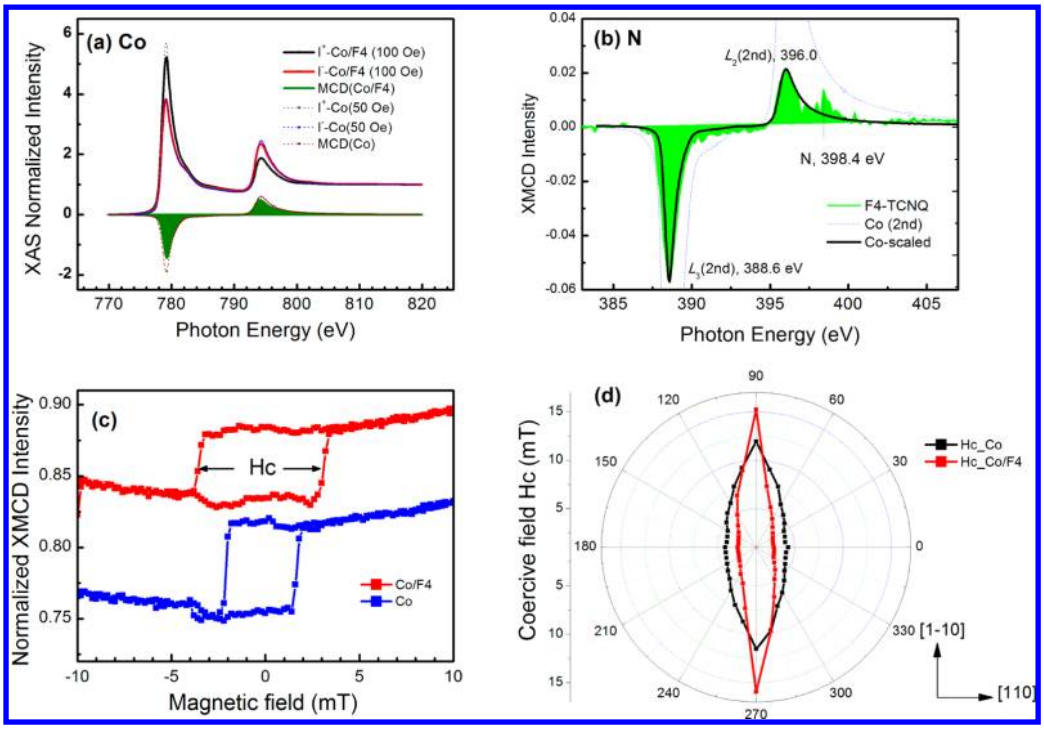

Figure 5. Enhanced anisotropic in-plane magnetization via hybridization-induced magnetic coupling. (a) Cobalt *L*-edge XAS for parallel (I^+) and antiparallel (I^-) orientation of the photon helicity with magnetic field and XMCD intensity ($I - I^+$) before and after F4-TCNQ adsorption. To avoid the interference from saturation field, a magnetic field, 5×10^{-3} T, was applied for bare Co film. (b) Nitrogen XMCD spectrum of F4-TCNQ (1.5 nm) on Co obtained from the intensity difference ($I^+ - I^-$) of parallel (I^+) and antiparallel (I^-) orientation of the photon helicity with magnetic field. The spectra were recorded in total-electron-yield mode near 300 K; the magnetic field was applied with alignment parallel ($\theta = 0°$) to the sample surface. (c) Hysteresis curve of bare Co and an F4-TCNQ overlayer obtained from the L_3 edge XMCD at 300 K. (d) Dependence on azimuthal angle of the coercive field measured with MOKE for bare Co and 2.0 nm F4-TCNQ on Co.

calculation, the spin-polarized DOS of Co suffers a slight decrease after molecule adsorption, an outcome consistent with the XMCD results in Figure 5a. The XMCD of N *K*-edge shown in Figure 5b demonstrates an observable positive intensity ($I^- - I^+$) line at 398.4 eV except 388.6 and 396.0 eV, which are mainly contributed from the second-order light of underlayer Co (denoted as $L_{2,3}$(second)). To eliminate the effect of second-order light, we have inserted two mirrors with high reflection for photon energy range near 400 eV but low for 800 eV, into the beamline. However, this led to low experimental signals due to the reduction of photon flux. To evaluate the background interference, the XMCD spectrum of Co shown in Figure 5a is rescaled in solid line and plotted with the XMCD spectrum of N in filled pattern for comparison. We found that whereas the N XMCD spectrum at 396.0 eV is satisfactorily fitted with L_2 (second), there is a non-negligible intensity difference at 398.4 eV. Apparently, CN is spin-polarized on the Co surface. The dichroic ratio of spin-polarized CN at 398.4 eV is estimated to be ca. 3%. The element-specific hysteresis loop measured from XMCD of Co L_3 edge for Co/F4-TCNQ as shown in Figure 5c has the form of a similar square loop, but the coercivity (H_c) is larger than that of the bare Co film. Because H_c is a measurement of anisotropy strength, its increased magnitude implies that the anisotropy of Co film is enhanced upon F4-TCNQ adsorption and can potentially produce a stronger magnetic order.[39] Because of the spin polarization of N XMCD at 398.4 eV and the enhanced coercivity of Co hysteresis loop, it implies adsorption-induced magnetic anisotropy via strong magnetic coupling between Co and F4-TCNQ.[39] To verify whether the easy axis is changed due to the molecular adsorption, we measured the angular dependence of magneto-optical Kerr effect (MOKE) ex situ. Although the Co is oxidized when exposed to air, we did not observe any polar signal for bare Co and Co/F4-TCNQ. Contrarily, the easy axis is still remained along [1−10] and [−110]. In Figure 5d, a remarkable enhancement of in-plane coercive field along the easy axis after F4-TCNQ deposition was obtained. The enhanced anisotropy observed on element-specific hysteresis loop and MOKE indicates that the stronger magnetic order might originate from the magnetic coupling between Co and CN of quasi-molecular magnet, which has a preferential orientation order and restructuring as shown above. This evidence strongly indicates that the spin polarization of F4-TCNQ via significant molecular restructuring yields an improved magnetic order at the interface that might facilitate the spin injection and transport in spintronic devices.

Our investigation demonstrates a conspicuous bidirectional charge transfer that produces significant molecular restructuring and thus induces organic magnetization through hybridization-induced magnetic coupling. The results suggest that the interfacial spin polarization is determined by the anchoring restructure. Such influential factors and correlations should be taken into account for fabricating spintronic devices. Moreover, the strong magnetic coupling produces a superior magnetic order at the organic−ferromagnetic interface. This tailored interface not only is capable of tuning energy levels with a surface dipole layer but also expresses an enhanced magnetic anisotropy, implying that restructuring-assisted spin polar-

dx.doi.org/10.1021/jz301757x | *J. Phys. Chem. Lett.* 2013, 4, 310−316

ization might shed light on the engineering of highly efficient spin injection and transport in organic spintronics.

EXPERIMENTAL METHOD

All experiments were manipulated in an ultrahigh-vacuum (UHV) system consisting of interconnected chambers for sample preparation and analysis with base pressure near 3×10^{-10} mbar. F4-TCNQ films of varied thickness were fabricated on Si (100)/Cr (3.4 nm)/Co (3.4 nm) substrates. The Co film with fcc (111) texturing[16,40] was grown from the vapor with a water-cooled electron-beam evaporator (Omicron EFM 3) on a substrate at a rate 0.2 nm min^{-1} of deposition assessed with a quartz-crystal microbalance (QCM). The organic F4-TCNQ, thoroughly degassed, was deposited through a Knudsen-cell evaporator. The average rate of deposition was measured with the QCM to be 0.1 nm min^{-1} at source temperature 380 K. All deposition was performed on a substrate near 300 K; the homogeneity of the film was inspected with synchrotron PES at various spots on the sample. We recorded PES at the 09A2 U5-spectroscopy and 08A1 LSGM beamlines in the National Synchrotron Radiation Research Center (NSRRC) in Taiwan for X-ray (XPS) and ultraviolet photoelectron spectroscopy (UPS), respectively. The polarized NEXAFS spectra were recorded at the photoelectron-emission microscope (PEEM) end station of beamline 05B2 EPU. The XMCD spectra were characterized at the 11A Dragon beamline provided by a bending source with circular polarization. Calculations were performed with the Vienna ab initio simulation program (VASP) using PAW-pseudopotential at the GGA-PW91 level.

ASSOCIATED CONTENT

Supporting Information

Details of our experimental apparatus, morphology of thin film examined with an AFM, spin-polarized DOS, total DOS of F4-TCNQ, and PDOS of CN either free or bound to Co, XMCD-based PEEM images, and MOKE measurements. This material is available free of charge via the Internet at http://pubs.acs.org.

AUTHOR INFORMATION

Corresponding Author

*E-mail: yjhsu@nsrrc.org.tw (Y.J.H.); jenghan@ntnu.edu.tw (J.H.W.).

Notes

The authors declare no competing financial interest.

ACKNOWLEDGMENTS

We thank Dr. Che-Wei Hsu for AFM measurements, Miss Diana Lin for valuable discussion, and Taiwan National Center for High-performance Computing (NCHC) for providing computational resources. National Science Council (NSC99-2113-M-213-002, NSC100-2113-M-213-002-MY2) and National Synchrotron Radiation Research Center partially funded this work.

REFERENCES

(1) Xiong, Z. H.; Wu, D.; Valy Vardeny, Z.; Shi, J. Giant Magnetoresistance in Organic Spin-Valves. *Nature* **2004**, *427*, 821−824.

(2) Yoo, J.-W.; Chen, C.-Y.; Jang, H. W.; Bark, C. W.; Prigodin, V. N.; Eom, C. B.; Epstein, A. J. Spin Injection/Detection Using an Organic-Based Magnetic Semiconductor. *Nat. Mater.* **2010**, *9*, 638−642.

(3) Gobbi, M.; Golmar, F.; Llopis, R.; Casanova, F.; Hueso, L. E. Room-Temperature Spin Transport in C60-Based Spin Valves. *Adv. Mater.* **2011**, *23*, 1609−1613.

(4) Sanvito, S. Molecular Spintronics. *Chem. Soc. Rev.* **2011**, *40*, 3336−3355.

(5) Dediu, V.; Hueso, L. E.; Bergenti, I.; Riminucci, A.; Borgatti, F.; Graziosi, P.; Newby, C.; Casoli, F.; De Jong, M. P.; Taliani, C.; Zhan, Y. Room-Temperature Spintronic Effects in Alq3-Based Hybrid Devices. *Phys. Rev. B* **2008**, *78*, 115203−115208.

(6) Santos, T. S.; Lee, J. S.; Migdal, P.; Lekshmi, I. C.; Satpati, B.; Moodera, J. S. Room-Temperature Tunnel Magnetoresistance and Spin-Polarized Tunneling through an Organic Semiconductor Barrier. *Phys. Rev. Lett.* **2007**, *98*, 016601−016604.

(7) Nguyen, T. D.; Sheng, Y.; Rybicki, J.; Veeraraghavan, G.; Wohlgenannt, M. Magnetoresistance in π-Conjugated Organic Sandwich Devices with Varying Hyperfine and Spin-Orbit Coupling Strengths, And Varying Dopant Concentrations. *J. Mater. Chem.* **2007**, *17*, 1995−2001.

(8) Sheng, Y.; Nguyen, T. D.; Veeraraghavan, G.; Mermer, Ö.; Wohlgenannt, M. Effect of Spin-Orbit Coupling on Magnetoresistance in Organic Semiconductors. *Phys. Rev. B* **2007**, *75*, 035202−035207.

(9) Nguyen, T. D.; Hukic-Markosian, G.; Wang, F.; Wojcik, L.; Li, X.-G.; Ehrenfreund, E.; Vardeny, Z. V. Isotope Effect in Spin Response of [pi]-Conjugated Polymer Films and Devices. *Nat. Mater.* **2010**, *9*, 345−352.

(10) Bobbert, P. A.; Wagemans, W.; van Oost, F. W. A.; Koopmans, B.; Wohlgenannt, M. Theory for Spin Diffusion in Disordered Organic Semiconductors. *Phys. Rev. Lett.* **2009**, *102*, 156604−156607.

(11) McCamey, D. R.; Seipel, H. A.; Paik, S. Y.; Walter, M. J.; Borys, N. J.; Lupton, J. M.; Boehme, C. Spin Rabi Flopping in the Photocurrent of a Polymer Light-Emitting Diode. *Nat. Mater.* **2008**, *7*, 723−728.

(12) Ruden, P. Organic Spintronics: Interfaces Are Critical. *Nat. Mater.* **2011**, *10*, 8−9.

(13) Schulz, L.; Nuccio, L.; Willis, M.; Desai, P.; Shakya, P.; Kreouzis, T.; Malik, V. K.; Bernhard, C.; Pratt, F. L.; Morley, N. A.; Suter, A.; Nieuwenhuys, G. J.; Prokscha, T.; Morenzoni, E.; Gillin, W. P.; Drew, A. J. Engineering Spin Propagation Across a Hybrid Organic/Inorganic Interface Using a Polar Layer. *Nat. Mater.* **2011**, *10*, 39−44.

(14) Barraud, C.; Seneor, P.; Mattana, R.; Fusil, S.; Bouzehouane, K.; Deranlot, C.; Graziosi, P.; Hueso, L.; Bergenti, I.; Dediu, V.; Petroff, F.; Fert, A. Unravelling the Role of the Interface for Spin Injection into Organic Semiconductors. *Nat. Phys.* **2010**, *6*, 615−620.

(15) Sanvito, S. Molecular Spintronics: The Rise of Spinterface Science. *Nat. Phys.* **2010**, *6*, 562−564.

(16) Chan, Y.-L.; Hung, Y.-J.; Wang, C.-H.; Lin, Y.-C.; Chiu, C.-Y.; Lai, Y.-L.; Chang, H.-T.; Lee, C.-H.; Hsu, Y. J.; Wei, D. H. Magnetic Response of an Ultrathin Cobalt Film in Contact with an Organic Pentacene Layer. *Phys. Rev. Lett.* **2010**, *104*, 177204−177207.

(17) Zhan, Y.; Holmström, E.; Lizárraga, R.; Eriksson, O.; Liu, X.; Li, F.; Carlegrim, E.; Stafström, S.; Fahlman, M. Efficient Spin Injection Through Exchange Coupling at Organic Semiconductor/Ferromagnet Heterojunctions. *Adv. Mater.* **2010**, *22*, 1626−1630.

(18) Tarafder, K.; Sanyal, B.; Oppeneer, P. M. Charge-Induced Spin Polarization in Nonmagnetic Organic Molecule Alq_3. *Phys. Rev. B* **2010**, *82*, 060413−060416.

(19) Javaid, S.; Bowen, M.; Boukari, S.; Joly, L.; Beaufrand, J. B.; Chen, X.; Dappe, Y. J.; Scheurer, F.; Kappler, J. P.; Arabski, J.; Wulfhekel, W.; Alouani, M.; Beaurepaire, E. Impact on Interface Spin Polarization of Molecular Bonding to Metallic Surfaces. *Phys. Rev. Lett.* **2010**, *105*, 077201−077204.

(20) Atodiresei, N.; Brede, J.; Lazicacute, P.; Caciuc, V.; Hoffmann, G.; Wiesendanger, R. Bl; uuml; gel, S. Design of the Local Spin Polarization at the Organic-Ferromagnetic Interface. *Phys. Rev. Lett.* **2010**, *105*, 066601−066604.

(21) Hofmann, O. T.; Egger, D. A.; Zojer, E. Work-Function Modification beyond Pinning: When Do Molecular Dipoles Count? *Nano Lett.* **2010**, *10*, 4369−4374.

(22) Zhou, X.; Blochwitz, J.; Pfeiffer, M.; Nollau, A.; Fritz, T.; Leo, K. Enhanced Hole Injection into Amorphous Hole-Transport Layers of Organic Light-Emitting Diodes Using Controlled p-Type Doping. *Adv. Funct. Mater.* **2001**, *11*, 310−314.
(23) Maennig, B.; Pfeiffer, M.; Nollau, A.; Zhou, X.; Leo, K.; Simon, P. Controlled p-Type Doping of Polycrystalline and Amorphous Organic Layers: Self-Consistent Description of Conductivity and Field-Effect Mobility by a Microscopic Percolation Model. *Phys. Rev. B* **2001**, *64*, 195208−195216.
(24) Romaner, L.; Heimel, G.; Brédas, J.-L.; Gerlach, A.; Schreiber, F.; Johnson, R. L.; Zegenhagen, J.; Duhm, S.; Koch, N.; Zojer, E. Impact of Bidirectional Charge Transfer and Molecular Distortions on the Electronic Structure of a Metal-Organic Interface. *Phys. Rev. Lett.* **2007**, *99*, 256801−256804.
(25) Rangger, G. M.; Hofmann, O. T.; Romaner, L.; Heimel, G.; Bröker, B.; Blum, R.-P.; Johnson, R. L.; Koch, N.; Zojer, E. F4TCNQ on Cu, Ag, and Au as Prototypical Example for a Strong Organic Acceptor on Coinage Metals. *Phys. Rev. B* **2009**, *79*, 165306−165317.
(26) Jain, R.; Kabir, K.; Gilroy, J. B.; Mitchell, K. A. R.; Wong, K.-c.; Hicks, R. G. High-Temperature Metal-Organic Magnets. *Nature* **2007**, *445*, 291−294.
(27) Kortright, J. B.; Lincoln, D. M.; Edelstein, R. S.; Epstein, A. J. Bonding, Backbonding, and Spin-Polarized Molecular Orbitals: Basis for Magnetism and Semiconducting Transport in $V[TCNE]_{x\sim2}$. *Phys. Rev. Lett.* **2008**, *100*, 257204−257207.
(28) Naaman, R.; Vager, Z. Cooperative Electronic and Magnetic Properties of Self-Assembled Monolayers. *MRS Bull.* **2010**, *35*, 429−434.
(29) Chiodi, M.; Gavioli, L.; Beccari, M.; Di Castro, V.; Cossaro, A.; Floreano, L.; Morgante, A.; Kanjilal, A.; Mariani, C.; Betti, M. G. Interaction Strength and Molecular Orientation of a Single Layer of Pentacene in Organic-Metal Interface and Organic-Organic Heterostructure. *Phys. Rev. B* **2008**, *77*, 115321−115327.
(30) Hu, W.-S.; Tao, Y.-T.; Chen, Y.-F.; Chang, C.-S. Orientation-Dependent Conductance Study of Pentacene Nanocrystals by Conductive Atomic Force Microscopy. *Appl. Phys. Lett.* **2008**, *93*, 053304−053303.
(31) Chen, W.; Chen, S.; Qi, D. C.; Gao, X. Y.; Wee, A. T. S. Surface Transfer p-Type Doping of Epitaxial Graphene. *J. Am. Chem. Soc.* **2007**, *129*, 10418−10422.
(32) Koch, N.; Duhm, S.; Rabe, J.; uuml; rgen, P.; Vollmer, A.; Johnson, R. L. Optimized Hole Injection with Strong Electron Acceptors at Organic-Metal Interfaces. *Phys. Rev. Lett.* **2005**, *95*, 237601.
(33) Aziz, E. F.; Vollmer, A.; Eisebitt, S.; Eberhardt, W.; Pingel, P.; Neher, D.; Koch, N. Localized Charge Transfer in a Molecularly Doped Conducting Polymer. *Adv. Mater.* **2007**, *19*, 3257−3260.
(34) Braun, S.; Salaneck, W. R. Fermi Level Pinning at Interfaces with Tetrafluorotetracyanoquinodimethane (F4-TCNQ): the Role of Integer Charge Transfer States. *Chem. Phys. Lett.* **2007**, *438*, 259−262.
(35) Fraxedas, J.; Lee, Y. J.; Jiménez, I.; Gago, R.; Nieminen, R. M.; Ordejón, P.; Canadell, E. Characterization of the Unoccupied and Partially Occupied States of TTF-TCNQ by XANES and First-Principles Calculations. *Phys. Rev. B* **2003**, *68*, 195115−195125.
(36) Stöhr, J.; Outka, D. A. Determination of Molecular Orientations on Surfaces from the Angular Dependence of near-Edge X-Ray-Absorption Fine-Structure Spectra. *Phys. Rev. B* **1987**, *36*, 7891−7905.
(37) Tseng, T.-C.; Urban, C.; Wang, Y.; Otero, R.; Tait, S. L.; Alcamí, M.; Écija, D.; Trelka, M.; Gallego, J. M.; Lin, N.; Konuma, M.; Starke, U.; Nefedov, A.; Langner, A.; Wöll, C.; Herranz, M. Á.; Martín, F.; Martín, N.; Kern, K.; Miranda, R. Charge-Transfer-Induced Structural Rearrangements at Both Sides of Organic/Metal Interfaces. *Nat. Chem.* **2010**, *2*, 374−379.
(38) Frazer, B. H.; Gilbert, B.; Sonderegger, B. R.; De Stasio, G. The Probing Depth of Total Electron Yield in the sub-keV Range: TEY-XAS and X-PEEM. *Surf. Sci.* **2003**, *537*, 161−167.
(39) Wende, H.; Bernien, M.; Luo, J.; Sorg, C.; Ponpandian, N.; Kurde, J.; Miguel, J.; Piantek, M.; Xu, X.; Eckhold, P.; Kuch, W.; Baberschke, K.; Panchmatia, P. M.; Sanyal, B.; Oppeneer, P. M.; Eriksson, O. Substrate-Induced Magnetic Ordering and Switching of Iron Porphyrin Molecules. *Nat. Mater.* **2007**, *6*, 516−520.
(40) Parkin, S. S. P.; Li, Z. G.; Smith, D. J. Giant Magnetoresistance in Antiferromagnetic Co/Cu Multilayers. *Appl. Phys. Lett.* **1991**, *58*, 2710−2712.